High-Frequency (95 GHz) EPR Spectroscopy To Characterize Spin Adducts

Tatyana I. Smirnova,*,§ Alex I. Smirnov,‡ R. B. Clarkson,†,‡ R. L. Belford,‡,§ Y. Kotake,⊥ and E. G. Janzen||

Illinois EPR Research Center, College of Veterinary Medicine and of Medicine and Department of Chemistry, University of Illinois at Urbana−Champaign, Urbana, Illinois 61801, Oklahoma Medical Research Foundation, Oklahoma, Oklahoma 73104, and Department of Clinical Studies, University of Guelph, Guelph, Ontario, Canada

Received: October 7, 1996; In Final Form: March 5, 1997[⊗]

EPR spin-trapping experiments are usually carried out at X-band (9.5 GHz) because of the good concentration sensitivity and ready availability of this method. The radical precursors are then characterized from an analysis of isotropic hyperfine coupling and comparison of these coupling factors with those for the reference spin adducts. These experiments encounter two major challenges: (i) spin adducts from many carbon-centered free radicals have *g* factors that are nearly the same (resulting in strongly overlapping spectra at 9.5 GHz), and (ii) measurable hyperfine couplings correspond to interactions of the electron spin with just the nearest nuclei. Therefore, very little or no information is obtained on the overall structure of the spin adduct molecule. Some of these difficulties can be overcome by carrying out spin-trapping experiments at 10-fold higher frequency, 95 GHz (W-band). Examples of two spin adducts with nearly the same isotropic *g* factors ($\Delta g_{iso} = 1.2 \times 10^{-4}$) are the benzene solutions of phenyl and trichloromethyl adducts of phenyl *tert*-butylnitrone (PBN). It is shown that, for a mixture of these spin adducts, the spectra from two species are resolved at W-band whereas the spectral lines severely overlap at X-band. For these spin adducts, additional line broadening at 95 GHz caused by an enhanced contribution from rotational modulation of the electronic **g** matrix is much too small to offset the gain in resolution due to Δg. It also is shown that parameters of rotational diffusion can be used to characterize spin adducts, even those with very similar local molecular structures and almost identical magnetic parameters, such as methyl-, ethyl-, and tetradecyl-PBN. These parameters are more accurately measured at W-band and characterize the spin adduct molecule as a whole. Multifrequency EPR data for toluene solutions of methyl- and tetradecyl-PBN show that the rotational diffusion of methyl-PBN is anisotropic with $\rho_x = 2.7 \pm 0.3$ and $\rho_y = 3.6 \pm 0.3$, while the rotation of tetradecyl-PBN is essentially isotropic with $\rho_x \approx \rho_y = 1.0 \pm 0.20$. The last indicates that the long alkyl chain of tetradecyl-PBN in solution is likely to be positioned around the nitroxide moiety, giving the molecule an effectively isotropic motion. Simulations of W-band EPR spectra from spin adducts with resolved proton hyperfine structure and analysis of motional data for these compounds in the absence of reliable data on anisotropic proton hyperfine couplings are also discussed.

Introduction

Over the past two decades, the spin-trapping technique has become a popular tool for detection and study of a variety of free radicals that could not have been observed directly by continuous-wave (CW) electron paramagnetic resonance (EPR) spectroscopy. In spin trapping, a free radical reacts with a spin trap, an unsaturated diamagnetic compound, to form a stable free radical, a spin adduct, that can be easily detected by EPR.[1] Spin trapping has been used to detect short-lived radicals and radicals with very short relaxation times, *e.g.*, hydroxy and superoxide radicals at low concentration.[2] These experiments are usually carried out with CW EPR spectroscopy at conventional frequency, 9.5 GHz (X-band), because of good concentration sensitivity (10^{-6}−10^{-7} M) and widespread availability of X-band facilities.

For most commonly used spin traps, the resulting spin adducts are fairly stable nitroxide radicals. Spin adducts are usually identified by a comparison of the magnitude of isotropic hyperfine coupling constants with those of reference nitroxides. Spin adducts that are unstable at ambient conditions can be stabilized by freezing. Principal axis components of anisotropic hyperfine coupling constants and *g* factors determined from frozen solution (rigid limit) EPR spectra can be also employed for spin adduct characterization.[3]

Identification of spin adducts encounters two major challenges: (i) spin adducts from many carbon-based free radicals have close *g* values ($\Delta g \approx 1 \times 10^{-3}$), which at X-band results in strongly overlapping spectra, and (ii) because of temperature, solvent, and concentration dependencies of the hyperfine coupling constants, the reference spectra must be recorded at exactly the same conditions as the spin adduct spectrum.[4] In many cases, the hyperfine coupling constants used for identification arise from nitrogen and β-hydrogen nuclei that belong to the spin trap itself. The hyperfine coupling constants may be affected just slightly by the nature of the reactive free radical attached to the spin trap, making conclusive identification of the radical precursor difficult. Several approaches have been introduced to improve this characterization by correcting the

† College of Veterinary Medicine.
‡ College of Medicine.
§ Department of Chemistry.
⊥ Oklahoma Medical Research Foundation.
|| University of Guelph.
* Address for correspondence: Box 16, 505 S. Mathews, Urbana, IL 61801. Tel (217)-244-2252, Fax (217)-333-8868, and E-mail Smirnova@rlb6000.scs.uiuc.edu.
⊗ Abstract published in *Advance ACS Abstracts,* April 15, 1997.

S1089-5647(96)03066-0 CCC: $14.00

data for experimental conditions and artifacts. For example, the use of the NoH parameter, which is defined as a ratio of nitrogen and β-hydrogen coupling constants and is independent of magnetic field scan, eliminates errors introduced by poor magnetic field calibration.[5] Solvent dependence of hyperfine coupling constants and correlation of those with solvent parameters like solvent acceptor number AN,[6] solvent polarity parameter $E_{T(30)}$,[7] and Kosower Z value[6,8] have been shown to be helpful in improving radical identification.

Hyperfine coupling constants measurable by CW EPR correspond to interaction with just the nearest nuclei. Combination of selective deuterium substitution of the spin trap with electron nuclear double-resonance spectroscopy (ENDOR) has been shown to be useful to probe long-range (*e.g.*, γ and δ) hyperfine interactions arising from the radical addend.[9,10] However, the hyperfine coupling constants may provide very little or no information on the overall structure and conformation state of the spin adduct molecule.

In this paper we examine how high-field (HF) EPR at 95 GHz (W-band) with enhanced g value resolution and sensitivity to rotational motion can provide additional information on spin adducts. Tenfold better g factor resolution at W-band than at conventional X-band allows us to clearly separate spectra arising from a mixture of spin adducts with close g factors, phenyl− and trichloromethyl−phenyl *N*-*tert*-butylnitrone (PBN), while the spectra from these two species almost completely overlap at X-band. Enhanced sensitivity of high-field EPR to rotational motion provides more accurate estimations of rotational dynamics parameters. These parameters characterize rotational motion of the spin adduct molecule as a whole and also can be used for differentiation of spin adducts, even those of very similar molecular structures such as methyl- and ethyl-PBN. It is also shown that principal components of rotational diffusion tensor as determined from multifrequency EPR and accurate 95 GHz g factor data report on configurations of spin adduct molecules in solution.

Materials and Methods

Spin Adduct Preparation. The trichloromethyl adduct of PBN was prepared, following a method reported by Janzen *et al.*,[11] from carbon tetrachloride, PBN, and α-nicotinide adenine dinucleotide phosphate reduced form (NADPH) with rat liver microsomal dispersions. The microsomal dispersion containing trichloromethyl adducts was extracted into a chloroform−methanol mixture. Subsequently, the adduct was purified by HPLC.[11] Phenyl, methyl, ethyl, and tetradecyl adducts of PBN were prepared in diethyl ether by the reaction between corresponding Grignard reagent (phenylmagnesium bromide, methylmagnesium bromide, ethylmagnesium bromide, or tetradecylmagnesium bromide) and PBN, followed by air oxidation.[9] PBN was synthesized at the facilities of the Oklahoma Medical Research Foundation. Grignard reagents were purchased from Aldrich (St. Louis, MO). The concentration of each spin adduct was estimated by EPR. Stock solutions of spin adducts were prepared in benzene.

Sample Preparation. For EPR measurements of rotational dynamics, aliquots of stock solutions of methyl-, ethyl-, and tetradecyl-PBN adducts in benzene were dried under nitrogen and then dissolved in toluene to the final spin adduct concentration (0.1 mM) in order to minimize the Heisenberg exchange. Toluene obtained from Aldrich (Milwaukee, WI) was additionally distilled. Quartz capillaries (i.d. = 0.7 mm, o.d. = 0.87 mm, length = 10 cm, VitroCom, Inc., Mountain Lakes, NJ) were custom-bent ("L-shape") to fit the experimental setup and flame-sealed at the short end. Solutions were drawn into the capillaries, deoxygenated by five freeze−thaw cycles, and then flame-sealed at the other end while the solutions remained frozen under liquid nitrogen. Solutions for X-band measurements were deoxygenated in the quartz sample tubes (i.d. = 3 mm, o.d. = 5 mm) in the same way.

For g value measurements at W-band, stock solutions of methyl- and tetradecyl-PBN adducts were dried under nitrogen flow, dissolved in toluene, methanol, and methanol−water (7:3 volume ratio) mixtures, and used without deoxygenation.

X-Band EPR Spectroscopy. EPR spectra at X-band were taken with a Varian (Palo Alto, CA) Century Series E-112 spectrometer equipped with a TE_{102} cavity and a Varian temperature controller (Model 906790). The magnetic field was calibrated by a tracking NMR Gaussmeter (Varian, Model 92980102P). Microwave frequency was measured by an online frequency counter (Systron Donner, Model 6016, Concord, CA). A small T-type (copper−constantan) thermocouple (Omega Engineering, Stamford, CT) was placed just outside the sensitive region of the cavity to prevent distortion of the EPR signal. Temperature was measured with an Omega Engineering (Model 410A1A) digital temperature indicator. During the measurements, temperature readings were stable and reproducible within ± 0.2 °C; however, the accuracy of temperature measurements at the sample site was estimated to be ±0.5 °C because of possible temperature gradients within the Dewar insert.[12] After temperature stabilization, the spectra were continuously recorded until no changes in line shape were observed. At each temperature, the last spectrum in the sequence was saved for further analysis.

Data acquisition was carried out by means of an IBM personal computer with an IBM analog−digital card, running a commercial software package (Scientific Software Services, Bloomington, IL).

W-Band EPR Spectroscopy. The W-band (94 GHz) spectrometer constructed at the University of Illinois EPR Research Center is described elsewhere.[13] A change from the previously described configuration[13,22,24] is that the magnetic field was supplied by an Oxford (Oxford Instruments, Inc., Concord, MA) custom-built 7 T superconductive magnet. The main superconductive coil of the magnet can be scanned and was set to approximately 3.36 T for this study. The magnetic field scan was provided by a water-cooled coaxial solenoid built at the University of Illinois. The sweeping coil was driven by a bipolar Techron (Techron Division of Crown International, Inc., Elkhart, IN) power supply amplifier which was modified by Mr. C. Reiner (Electronic Services, School of Chemical Sciences, University of Illinois) to accommodate a custom-engineered precision feedback circuit based on an Ultrastab 860R sensor (Danfysik, Jyllince, Denmark, and GMW Associates, Redwood City, CA) for inductive measurements of the current through the coil, with linearity better than 5 ppm and resolution of 0.05 ppm. This scanning system provided a variable scan/offset up to ±550 G from the main field under digital (15 bits resolution) computer control. Incorporation of the Ultrastab transducer into the control circuitry significantly improved stability and linearity of the current during the scan (better than 20 ppm over ±17 A). For studies of very narrow lines when the digital resolution might be limited, the system allows an analog external ramp. Tests carried out with deoxygenated solutions of perdeuterated nitroxide Tempone (2,2′,6,6′-tetramethyl-4-piperidone 1-nitroxide; Cambridge Isotope Laboratories, Inc., Andover, MA) demonstrated that the overall inhomogeneity of this magnet system is better than 20 mG over the sample region (within central 200 G scan of the water-cooled coil).

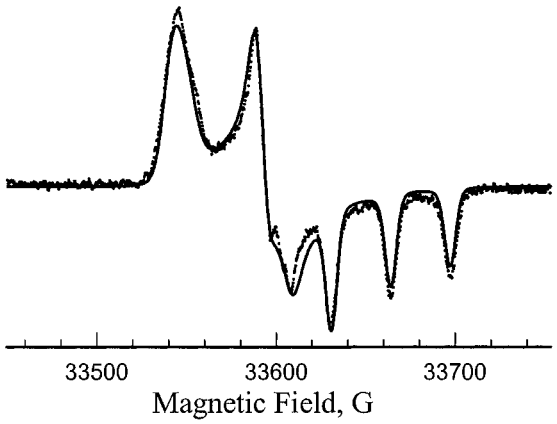

Figure 1. The 95 GHz EPR rigid limit spectrum of 1 mM toluene solution of methyl-PBN spin adduct obtained at −150 °C (small dots) is superimposed with results of least-squares simulation (solid line). The best-fit magnetic parameters are given in Table 1.

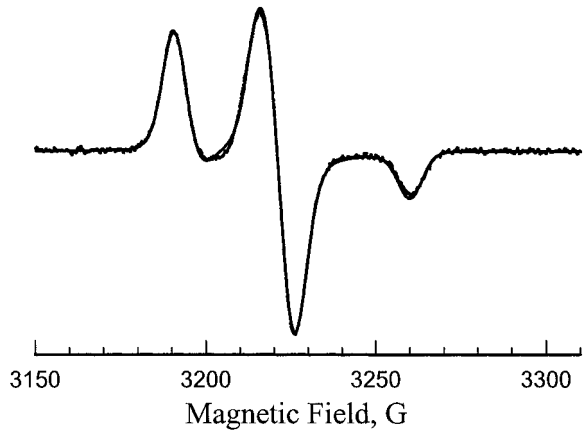

Figure 2. The 9.5 GHz EPR rigid limit spectrum of 1 mM toluene solution of methyl-PBN spin adduct obtained at −150 °C (small dots) is superimposed with results of least-squares simulation (solid line). The best-fit magnetic parameters are consistent with those obtained from 95 GHz fit and are listed in Table 1.

The scan and the center of magnetic field were calibrated with a Metrolab precision NMR teslameter PT 2025 (GMW Associates, Redwood City, CA). The microwave frequency was assured with a source-locking microwave counter (Model 578, IEP Microwave Inc., San Jose, CA). The cavity was a cylindrical type TE_{01n} ($n = 2$, 3 depending upon tuning) made of a gold foil (0.025 mm thick, purchased from Alfa Aesar, Ward Hill, MA) on a quartz support. The quality factor of the unloaded cavity is 4000. The cavity was fixed inside a brass waveguide block, which provides excellent mechanical and thermal stability. Microwave detection was provided by a tunable Shottky diode (Hughes Aircraft Co., Microwave Products Division, Torrance, CA) with a low-noise preamplifier and a bias current supply. A lock-in amplifier SR-530 (Stanford Research Systems, Inc., Sunyvale, CA) was used for phase-sensitive detection at 100 kHz magnetic field modulation. The sample temperature was monitored by two Fluke digital thermometers (Model 51, Fluke, Palatine, IL) equipped with miniature K-type (aluminum−nickel alloy) thermocouples fixed inside the upper and lower parts of the microwave cavity block. For cooling the system below room temperature, flowing nitrogen gas was passed through a heat exchanger placed in a Dewar with liquid nitrogen and then through a standard Varian variable temperature insert into the insulated line to cool the whole cavity assembly. An alternative variable-temperature system was outfitted with a modified constant flow CF1200 cryostat, an AutoGFS transfer line, and an ITC-4 digital temperature controller (all supplied by Oxford Instruments Inc., Concord, MA). We considered temperature of the sample stable if the readings of both thermometers were the same within the measurement accuracy, ±0.1 °C. Stability of the resonance frequency of the cavity (±25 kHz) during the measurement served as another indication of temperature stability. As in the X-band experiments, EPR spectra were taken until no changes were observed, the last spectrum in each sequence being saved for analyses.

Determination of Magnetic Tensor Parameters. Rotational motion of the radicals can be analyzed if their magnetic parameters are measured accurately, for example, from the rigid limit (or "powder pattern") EPR spectrum. As has been shown,[14] these measurements are more accurate at very high EPR frequencies (>90 GHz) because of the enhanced g factor resolution. Principal axis components of both nitrogen hyperfine and **g** matrices for methyl- and tetradecyl-PBN spin adducts were measured from the 94.3 and 9.5 GHz near rigid limit spectra ($T = -150$ °C) of 1 mM toluene solution (Figures 1 and 2). The initial correction for the observed microwave phase shift at 95 GHz was accomplished in a way similar to that described by Budil *et al.*[21] Corrected 95 GHz spectra were simulated with the HPOW computer program (Illinois EPR Research Center), available by anonymous FTP from World Wide Web site http://ierc.scs.uiuc.edu. The **g** and nitrogen hyperfine matrix (**A**) principal axis components and the anisotropic line width were defined by a SIMPLEX least-squares optimization procedure.[16] Values of x and y components of the nitrogen hyperfine matrix are difficult to measure directly from the experimental 94.3 GHz spectrum, since the corresponding lines are not or poorly resolved because of proton superhyperfine and/or "g strain" broadening at this frequency. At lower frequencies (*e.g.*, X-band), "g strain" effects should be negligible. In order to check the consistency of the simulation, we measured the rigid limit spectra ($T = -150$ °C) for the same samples at X-band (Figure 2) and repeated the simulation adjusting only principal axis components of the **A** matrix, the line widths, and the isotropic g factor; the **g** anisotropy was the same as from the W-band fit. The isotropic g factor was adjusted over a small range (corresponding to <1 G at X-band) to account for differences in magnetic field calibration between the two spectrometers. The result of the fit (Figure 2) demonstrates that our simulations at both W- and X-band are consistent. Corresponding magnetic parameters are listed in Table 1.

In the fast motional limit, EPR spectra from all spin adducts studied have shown a well-resolved splitting of nitrogen hyperfine components by hyperfine interaction with β-hydrogen. However, even at X-band, lines corresponding to β-hydrogen principal axis orientations were not resolved for both slowly and rapidly frozen toluene solutions. We have also observed the three principal axis orientations to have the same line width. That may serve as an indication that the anisotropy of the β-hydrogen is moderate or small. Also, although data on anisotropic β-hydrogen hyperfine coupling parameters for PBN spin adducts seem to be absent in literature, rigid limit spectra of DMPO spin adducts have shown that this coupling has very little anisotropy.[3]

Results and Discussion

Characterization of Spin Adducts in Mixture. A major established advantage of high-field EPR spectroscopy is in enhanced g factor resolution.[15] The ability to resolve two spectra from a mixture of different spin adducts is defined by the difference in the field position of the spectra ΔH:

TABLE 1: Magnetic Parameters Measured from Rigid Limit EPR Spectra of Spin Adducts in Toluene

	methyl-PBN	tetradecyl-PBN		methyl-PBN	tetradecyl-PBN
g_x	$2.00934 \pm 3 \times 10^{-5}$	$2.00933 \pm 3 \times 10^{-5}$	A_x/γ_e[c]	4.48 ± 0.2 G	4.08 ± 0.2 G
g_y	$2.00619 \pm 3 \times 10^{-5}$	$2.00617 \pm 3 \times 10^{-5}$	A_y/γ_e	6.64 ± 0.2 G	5.84 ± 0.2 G
g_z	$2.00234 \pm 3 \times 10^{-5}$	$2.00237 \pm 3 \times 10^{-5}$	A_z/γ_e	33.40 ± 0.2 G	33.66 ± 0.2 G
$\langle g \rangle$[a]	$2.00596 \pm 5 \times 10^{-5}$	$2.00596 \pm 5 \times 10^{-5}$	$\langle A \rangle/\gamma_e$[d]	14.84 ± 0.3 G	14.53 ± 0.3 G
g_{iso}[b]	2.00601	2.00597	a_{iso}/γ_e	14.83 G	14.54 G

[a] $\langle g \rangle = {}^1/_3(g_x + g_y + g_z)$. [b] Measured from fast-motion spectra at 94 GHz. [c] γ_e is the magnetogyric ratio of the free electron. [d] $\langle A \rangle = {}^1/_3(A_x + A_y + A_z)$.

$$\Delta H \approx (h\upsilon/g_{el}{}^2\beta)\Delta g \qquad (1)$$

and the line width $\Delta H_{p-p}(\upsilon)$ at a given resonance frequency υ. Most carbon-centered spin adducts have close g factors ($\Delta g < 1 \times 10^{-3}$) and nitrogen hyperfine coupling parameters. As a result, mixtures of different spin adducts formed by the same spin trap are likely to give strongly overlapping spectra at conventional EPR frequencies (8.8−9.5 GHz). Figure 3A shows an X-band (9.5 GHz) spectrum from a mixture of phenyl- and trichloromethyl-PBN adducts in benzene at 24 °C. Only the high-field line ($m_I = -1$ nitrogen hyperfine component) has some small extra broadening on the line shoulder (shown by an arrow) which might be an indication of a presence of two species. This strong overlap of the X-band spectra makes an accurate determination of the number of species as well as nitrogen and β-hydrogen hyperfine coupling parameters a difficult task. Figure 3B shows the 94.5 GHz EPR spectrum from the same mixture of spin adducts at the same temperature. Because spectral separation ΔH is proportional to the resonance frequency υ at the same Δg, the presence of two radical adducts becomes clear at W-band. Increase in microwave frequency also results in broader lines at 95 GHz because of enhanced contributions to the line width $\Delta H_{p-p}(\upsilon)$ from the spectral densities arising from rotational modulation of the electronic **g** matrix.[21] However, as can be seen from the spectrum, the line broadening at 95 GHz is much too small to defeat the gain in resolution due to Δg. A more detailed discussion of this issue is given in the next section of this paper.

To measure hyperfine parameters of the spin adducts present in the mixture, the 95 GHz spectrum was simulated as a superposition of two signals with different hyperfine splittings on nitrogen and β-hydrogen nuclei. A Voigt function (convolution of Lorentzian and Gaussian functions) with different homogeneous line width was assigned to each of the nitrogen hyperfine components. A fitting program, based on a fast convolution algorithm with a Levenberg−Marquardt optimization method,[17] was employed to extract g factors as well as nitrogen and hydrogen hyperfine coupling parameters directly from the experimental spectrum. The best-fit results and corresponding EPR spectra from individual spin adducts are shown in Figure 3B−D (simulated mixture spectrum, phenyl- and trichloromethyl-PBN adducts, respectively). Spectral parameters and predicted parameter uncertainties obtained by the fitting procedure are summarized in Table 2 (mixture 1). To check uniqueness of the fit and validity of the measured hyperfine coupling constants, we have measured and least-squares simulated a 95 GHz spectrum from a mixture of the same spin adducts, but with the concentration ratio reversed from that in mixture 1 (simulated spectra not shown). This experiment is referred to as mixture 2 in Table 2. Spectral parameters obtained in both experiments are the same within the predicted uncertainties. Measured hyperfine parameters are in good agreement with those determined for individual spin adducts in earlier experiments carried out with benzene as a solvent.[18]

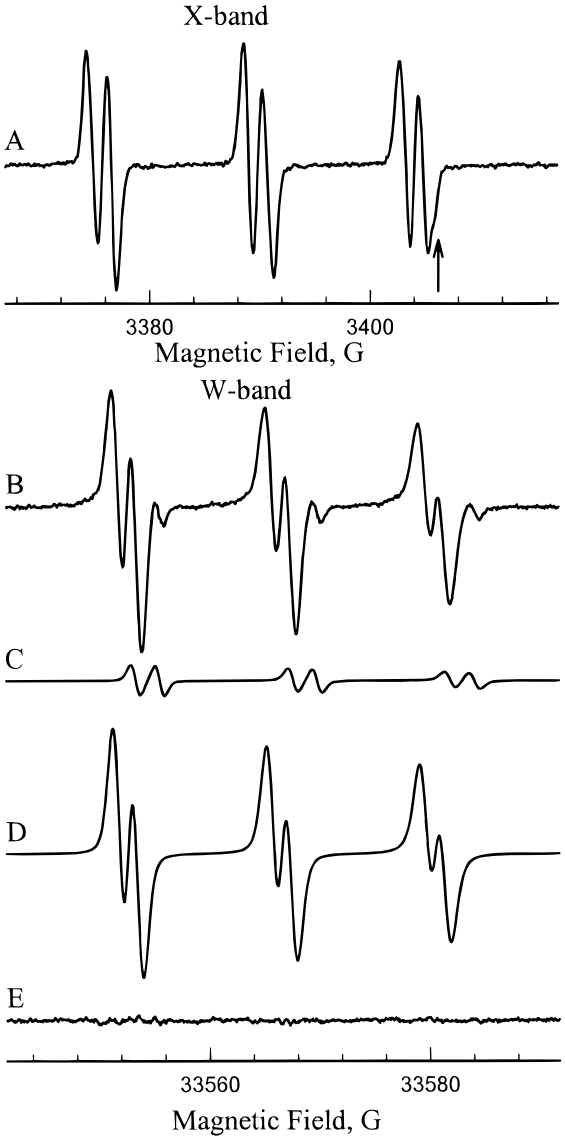

Figure 3. (A) X-band (9.5 GHz) EPR spectrum from a mixture of phenyl-PBN and trichloromethyl-PBN adducts in benzene at 24 °C. Arrow points to some extra broadening on the line shoulder which is caused by the presence of two species. (B, C, D) Experimental W-band (95 GHz) spectrum of the mixture and the corresponding least-squares-simulated spectra of phenyl-PBN and trichloromethyl-PBN adducts, respectively. Nitrogen hyperfine coupling parameters determined by simulation are given in Table 2. (E) Residual; difference between experimental (B) and simulated spectra (C, D).

Our experiments show that HF (95 GHz) EPR can be applied successfully for characterization of spin adducts in a mixture: individual EPR spectra of spin adducts even with a small Δg ($\approx 1.2 \times 10^{-4}$) are separated while the spectral lines severely overlap at X-band (9.5 GHz). For these spin adducts additional line broadening at 95 GHz is much too small to offset the gain in resolution due to Δg.

TABLE 2: Isotropic Magnetic Parameters of Phenyl-PBN (1) and Trichloromethyl-PBN (2) Spin Adducts from Mixtures of Benzene Solutions As Measured at 94.5 GHz

mixture 1	mixture 2	mixture 1	mixture 2
$g_{iso}(1) = 2.00614$	$g_{iso}(1) = 2.00614$	$g_{iso}(2) = 2.00626$	$g_{iso}(2) = 2.00626$
$a_N(1)/\gamma_e = 14.263 \pm 0.002$ G	$a_N(1)/\gamma_e = 14.266 \pm 0.002$ G	$a_N(2)/\gamma_e = 13.878 \pm 0.001$ G	$a_N(2)/\gamma_e = 13.882 \pm 0.001$ G
$a_H(1)/\gamma_e = 2.148 \pm 0.004$ G	$a_H(1)/\gamma_e = 2.143 \pm 0.004$ G	$a_H(2)/\gamma_e = 1.540 \pm 0.012$ G	$a_H(2)/\gamma_e = 1.530 \pm 0.012$ G

Rotational Dynamics of PBN Spin Adducts. Identification of radical precursors becomes even more challenging when the formed spin adducts have a similar or identical structure in the close vicinity of the unpaired electron. Examples of this include PBN spin adducts formed from alkyl radicals with variable chain length. We have measured magnetic parameters for two very different alkyl PBN spin adducts—methyl and tetradecyl in a nonpolar solvent toluene—and found these parameters almost identical (Table 1). Thus, magnetic parameters alone might be insufficient for radical precursor identification. (Of course, the methyl spin adduct could be identified from the three protons of the methyl group, but detection of more remote protons for other alkyl spin adducts is complicated.) However, dynamic parameters measured from W-band spectra of these two adducts in fast motion limit were strikingly different, indicating very different rotational correlation time and rotational radii. This dynamic behavior of the spin adducts has been further studied at various temperatures using carefully deoxygenated samples.

In the fast motion limit, the homogeneous line width depends upon nuclear spins. Usually, for many nitroxides, the proton hyperfine interactions are neglected in the spectral analysis; however, for most PBN spin adducts $a^{H}_{iso}/a^{N}_{iso} \approx 0.2$, and the line width dependence upon m_H should be also taken into consideration. Then, the homogeneous line width for each of six hyperfine components can be written as[23]

$$T_2^{-1} = A + B_N m_N + C_N m_N^2 + B_H m_H + C_H m_H^2 + D m_N m_H \quad (2)$$

where A, B_i, C_i, and D (i = N, H) are the line width parameters expressed in terms of spectral densities. This system of equations, as applied to PBN spin adducts, can be solved for line width parameters; however, two line width parameters, A and $^1/_4C_H$, are determined only as their sum ($A + {}^1/_4C_H$). This term also includes frequency-independent contributions to T_2 such as spin−rotational coupling and Heisenberg spin exchange which are often denoted as A'.

Secular spectral densities contributing to the line width parameters A, B, and C have very different frequency dependence. For example, at 94 GHz the line width parameter C_N remains approximately the same as at 9.5 GHz, because the contributing secular spectral density arises from the rotational modulation of the nitrogen hyperfine tensor and is frequency independent. Parameter B_N is determined primarily by a correlated modulation of both **g** and **A** matrices and therefore is approximately proportional to the resonance frequency υ (if pseudosecular and nonsecular spectral densities are neglected). Parameter A_N is enhanced the most at the high fields because it contains the secular spectral density J^{GG}, arising solely from the rotational modulation of the electronic **g** matrix, which increases as υ^2. Although this spectral density at W-band is larger by a factor of 100 than at X-band, the peak-to-peak width of the $m_N = 0$ nitrogen transition, as can be seen from Figure 3, is increased only moderately. One reason for this is that at X-band the homogeneous width of the $m_N = 0$ line is dominated by rotational modulation of the hyperfine tensor and also contains frequency-independent contributions (denoted as A') such as spin−rotation coupling and Heisenberg spin exchange. The relative contribution from the electronic **g** matrix spectral density J^{GG} is rather small. As an example, we have calculated ($A - A'$) and J^{GG} for methyl-PBN spin adduct solution in toluene, using the theory of motionally narrowed EPR spectra at high EPR fields[21,22] and the experimental anisotropy parameters, as will be derived below. At 9.05 GHz (X-band) and $T = 260$ K, the contribution from rotational modulation of the nitrogen hyperfine matrix is ($A - A'$) = 20.4 mG while the contribution from the electronic **g** matrix spectral density is almost negligible ($J^{GG} = 1.0$ mG). At 94.5 GHz (W-band), the line width parameter ($A - A'$) is 121 mG and is dominated by J^{GG} (=107 mG). Thus, although J^{GG} is increased more than 100-fold, the overall broadening of the $m_N = 0$ line for this viscosity/temperature arising solely from the rotational modulation of **g** matrix is only about 100 mG.

The second reason for only a very moderate line broadening for this spin adduct at W-band is a large inhomogeneous line width (≈1 G), as is typical of many nondeuterated nitroxide spin-labels and spin adducts. The inhomogeneous line width caused by unresolved and partially resolved hydrogen hyperfine interactions is typically about 0.6−1.0 G. Thus, for solutions of methyl-PBN adduct in nonviscous solvents, the inhomogeneous broadening dominates the line width at both X- and W-bands. Then the relative broadening of the $m_N = 0$ transition for these and many other nondeuterated spin adducts at W-band EPR frequency is expected to be quite moderate (≲20%; about 10% for methyl-PBN), while the difference in the field position ΔH between species with different **g** factors proportionally increases with the EPR frequency υ (see eq 1). This explains the substantial gain in spectral resolution at high magnetic fields that makes HF EPR an exceptional tool to separate spin-label EPR spectra arising from phases with a different polarity[24] or to characterize the spin adducts from the mixtures, as demonstrated above. For methyl-PBN in toluene and $T = 260$ K, J^{GG} becomes comparable with the inhomogeneous width (≈1 G) only at ≈300 GHz; thus, even greater spectral resolution should be achievable at EPR frequencies higher than W-band.

Secular spectral densities increase proportionally with the rotation correlation time τ_R, and the relative line width broadening at W-band will also increase with the increase of the viscosity-to-temperature ratio. Estimates show that the gain in spectral resolution at W-band disappears only when the HF EPR spectrum falls into an intermediate motional regime.

As was emphasized recently,[20−22] the line width parameters measured at X-band contain different information on the rotational diffusion tensor **R** from those measured at higher EPR fields, *e.g.*, 95−250 GHz, because of a different symmetry of dominating magnetic matrices **g** and **A**. At X-band, the line width parameters B_N and C_N are dominated by rotational modulation of the nitrogen hyperfine tensor $\mathbf{A}_N$. This imposes a linear constraint on the principal values of rotational diffusion tensor **R**:

$$\rho_x = \alpha\rho_y + \beta \quad (3)$$

where $\rho_i = R_i/R_z$, $i = x, y$; the constants α and β are functions of B_N/C_N, principal values of $\mathbf{A}_N$ and **g** matrices, and the magnetic field.[23] Constraint (3) is also known as an allowed-value equation (AVE). Parameters B_N and C_N can be determined from solving the system of eqs 2.

At high magnetic fields ($H \gtrsim 1.8$ T, $\upsilon \gtrsim 50$ GHz) a new independent AVE (similar to (3)) can be obtained from another ratio of magnetic parameters A/B_N. Parameter A at these magnetic fields is dominated by the rotational modulation of **g** matrix, which has a different symmetry from **A**.[20,21] Two independent AVE's make determination of full rotational diffusion tensor of the radical possible.[21]

At $\upsilon \gtrsim 50$ GHz, the line width parameters A and B_N dominate over C_N because of enhanced contribution from rotational modulation of the electronic **g** matrix. For PBN spin adducts, parameter A measured at 95 GHz includes also spectral densities arising from rotational modulation of nitrogen $\mathbf{A}_N$ and β-proton $\mathbf{A}_H$ hyperfine coupling. However, contributions from these nonsecular densities in many cases could be neglected. Indeed, we have shown that for 95 GHz nonsecular terms arising from rotational modulation of nitrogen hyperfine matrix $\mathbf{A}_N$ become negligible at rotational correlation time $\tau_R \geq 20 \times 10^{-12}$ s or $B_N \geq 0.10$ G.[22] Anisotropy of $\mathbf{A}_H$ is likely to be smaller than $\mathbf{A}_N$ (*e.g.*, see ENDOR data on proton hyperfine of other nitroxide radicals reported in refs 3 and 25), and therefore corresponding nonsecular terms are even smaller than those determined by $\mathbf{A}_N$. Thus, when nonsecular terms arising $\mathbf{A}_N$ can be neglected, the $\mathbf{A}_H$ terms can be neglected as well.

For PBN spin adducts, parameters A and C_H cannot be separated by solving eq 2 without additional experiments on isotopically substituted molecules, similar to experiments carried out with nitroxide radicals containing ^{16}O and ^{17}O.[23,26] Without data on PBN adducts deuterated at the β hydrogen, only the sum ($A + {}^1/_4C_H$) can be measured. However, line width parameter C_i (i = H for hydrogen and i = N for nitrogen) contains only spectral densities arising from rotational modulation by hyperfine tensor. At 95 GHz, parameter C is much smaller than A and B. For example, for a typical nitroxide radical at this frequency, $C_N/A \approx 0.07$.[22] Taking into account even smaller anisotropy for the $\mathbf{A}_H$ matrix, one gets from even a very conservative estimate ${}^1/_4C_H < 0.01A$, so the contributions from $\mathbf{C}_H$ to line width parameter A are comparable with the experimental error and can also be neglected. For EPR frequency higher than 95 GHz, relative contribution to the spectral densities arising from rotational modulation of β-hydrogen hyperfine tensor will be even smaller.

The 9.5 and 94.5 GHz EPR data were analyzed by fitting each of six components of the experimental spectrum to the following fitting function:

$$F(B) = [p_1(B,\Delta B^G) * p_2(B,a^n) * m(B,\alpha_j)]k_1B + k_0 \qquad (4)$$

where $p_1(B,\Delta B^G)$ is a Gaussian envelope, $p_2(B,a^n)$ is the γ-proton hyperfine envelope with coupling constant a^n for n equivalent protons ($n = 3$ for methyl-PBN and $n = 2$ for tetradecyl-PBN), $m(B,\alpha_j)$ is a Lorentzian line shape function (α_j are the line shape parameters such as peak-to-peak width ΔB^L_{p-p}, microwave phase shift $\Delta\varphi$, and intensity), and * represents the convolution operator.[17] The line widths of the Gaussian envelope, microwave phase shift $\Delta\varphi$, and double integrated intensity were assumed to be the same for all six lines. Hyperfine coupling factors for γ-hydrogens and the largest ^{13}C couplings were determined by least-squares computer simulation of the X-band spectra, where the hyperfine structure is partially resolved. During the fitting of 94.5 GHz spectra these hyperfine coupling factors were not adjusted.

Figure 4A shows an experimental W-band EPR spectrum of 0.1 mM solution of tetradecyl-PBN adduct in toluene at 6 °C. The best-fit simulated spectrum with Lorentzian line width optimized independently for each of six hyperfine components is superimposed with the experimental data; the residual is shown in Figure 4B. Accounting for motion-modulated contributions from β-hydrogen to the line width is important for accurate fitting of the data. When this contribution was neglected (*i.e.*, the same Lorentzian line width was assumed for both lines in β-hydrogen doublets), the residual norm of the best least-squares fit increased by ≈50%, and deviations between the fit and the experiment became visible in the residual (Figure 4C).

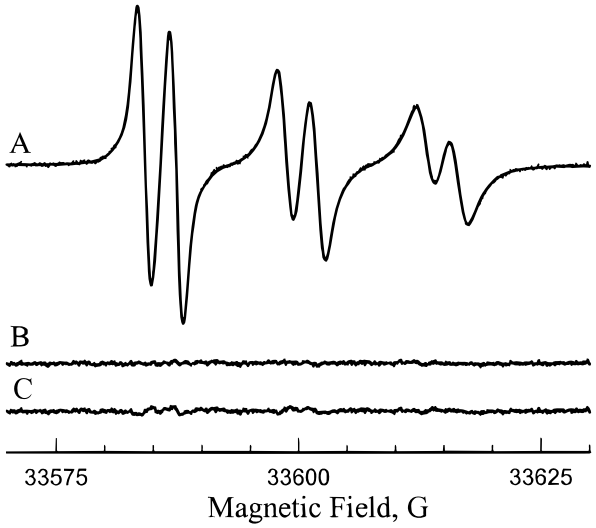

Figure 4. (A) Experimental W-band (95 GHz) EPR spectrum from 0.1 mM solution of tetradecyl-PBN adduct in toluene at 6 °C (shown as small dots) is superimposed with least-squares-simulated spectrum (solid line); Lorentzian line width for each of six spectral components have been optimized independently. The residual (B) shows no visible deviations between the experiment and the fit. (C) is the residual of least-squares fit according to a model which neglects contribution of β-hydrogen to the line width, *i.e.*, assuming the same Lorentzian line width for both lines in the β-hydrogen doublets.

The relative effect of β-hydrogen hyperfine coupling on motionally modulated homogeneous line width at multiple EPR frequencies is easy to consider by looking at the central doublet. The difference between two hydrogen components of the $m_N = 0$ transition is equal to the line width parameter B_H. This parameter contains contributions from spectral densities arising from a correlated effect of rotational modulation of both **g** and $\mathbf{A}_H$ matrices. Thus, the difference between the homogeneous widths of these two components increases proportionally with the magnetic field. For example, at $T = 250$ K, which corresponds to the middle of the temperature interval studied, $B_H^{94.5} = 42 \pm 8$ mG while $B_H^{9.5} = 4 \pm 3$ mG. Although the absolute value of $B_H^{9.5}$ is typically low and the relative error for this parameter is high from X-band measurements, the line width dependence upon the β-hydrogen quantum number cannot be neglected because of a measurable value of $C_H^{9.5}$.

It has been previously emphasized for X-band EPR frequencies that accurate measurements of rotational motion of the spin probes with a relatively large superhyperfine structure require data on proton hyperfine matrices from, for example, ENDOR experiments.[25] As expected, at 95 GHz the spectrum of such nitroxides is primarily determined by the rotational modulation of the anisotropic **g** factor, and anisotropic proton hyperfine data might be not necessary. At these frequencies, the only measurable line width parameter related to the proton hyperfine is B_H; however, its contribution to the homogeneous width can be separated as described above. Thus, at W-band the motion of spin adducts can be accurately analyzed without anisotropic proton hyperfine data.

Experimental W- and X-band spectra over the temperature range from 20 to −70 °C were fitted in automatic mode, and

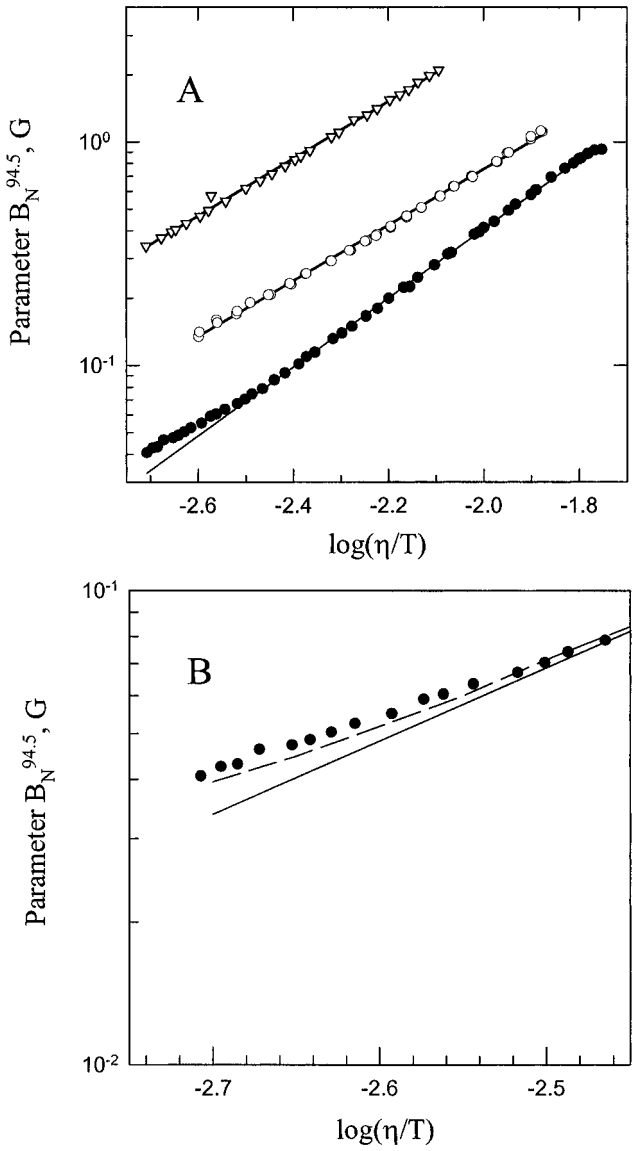

Figure 5. (A) A log−log plot of W-band (94.5 GHz) line width parameter $B_N^{94.5}$ for 0.1 mM solutions of methyl-PBN (closed circles), ethyl-PBN (open circles), and tetradecyl-PBN (open triangles) in toluene measured as functions of viscosity-to-temperature ratio. Abscissa is log-(η/T), where η/T is in cP K^{-1}. Results of first-order regressions of the linear portions of the curves are shown as solid lines. (B) A portion of $B_N^{94.5}$ methyl-PBN (closed circles) data corresponding to low viscosity-to-temperature ratios. Solid line is the contribution from the secular spectral density only. Dashed line is a theoretical curve for the model of anisotropic Brownian diffusion with the anisotropy parameters $\rho_x = 2.7 \pm 0.3$ and $\rho_y = 3.6 \pm 0.3$, which includes the nonsecular terms.

the results were used to calculate line width parameters $B_N^{9.5}$, $C_N^{9.5}$ at 9.5 GHz and $A^{94.5}$, $B_N^{94.5}$ at 94.5 GHz through the system of eqs 2. Figure 5A shows line width parameter $B_N^{94.5}$ (on a logarithmic scale) as a function of the logarithm of viscosity-to-temperature ratio (η/T) as measured at W-band for methyl-PBN and tetradecyl-PBN spin adducts. For the same magnetic and anisotropy parameters, the value of B_N is proportional to the rotational correlation time τ_R if the contributions from nonsecular and pseudosecular spectral densities can be neglected ($B_N^{94.5} \gtrsim 0.1$ G). Thus, the data shown in Figure 5A indicate very different rotational motions of the two spin adducts at the same η/T ratio, with the tetradecyl-PBN exhibiting a slower overall motion than the much smaller methyl-PBN.

The line width parameter B_N increases linearly with magnetic field. As a result, any difference between line width parameters B_N measured at the same η/T for two spin adducts with different τ_R increases with EPR frequency. For example, the difference in parameters B_N measured at $T = 250$ K for these two spin adducts is about 0.88 ± 0.01 G at 94.5 GHz compared to 0.09 ± 0.01 mG at 9.5 GHz. Clearly, the accuracy is higher at W-band. The methyl- and tetradecyl-PBN spin adducts have a widely differing molecular structure and molecular weight and therefore are expected to show a difference in rotational dynamics. To check whether the HF EPR is capable of separating spin adducts of similar weight/structure, another compound, ethyl-PBN, was chosen. Experimental data were collected for the same solvent, toluene, and over a similar temperature range. The plot of parameter $B_{N94.5}$ for ethyl-PBN shown in Figure 5A demonstrates that the motion of ethyl-PBN is different from a similar compound, methyl-PBN. Overall, the plot of $B_{N94.5}$ for ethyl-PBN falls in between the curves for methyl- and tetradecyl-PBN. This experiment demonstrates that HF EPR is capable of differentiating even quite similar PBN spin adducts by motional parameters.

Figure 5A shows that for ethyl- and tetradecyl-PBN spin adducts, the parameter $B_N^{94.5}$ is proportional to η/T in the log−log plot over the whole temperature range studied. (Linear regression is shown as a solid line.) For methyl-PBN, $B_N^{94.5}$ deviates noticeably from linearity at low viscosity-to-temperature ratios ($\eta/T < 10^{-2.45}$ cP K^{-1}) because of nonnegligible contributions from the nonsecular spectral densities. Figure 5B shows only a portion of the $B_N^{94.5}$ data for a very fast tumbling rate of the methyl-PBN. The solid line corresponds to the contribution from the secular spectral density only. The dashed line, which is a theoretical $B_N^{94.5}$ curve for the model of anisotropic Brownian diffusion and which includes the nonsecular terms, closely follows the experimental data. It is apparent that at the fastest tumbling rates the theoretical curve is slightly lower than the experimental values. We judge this deviation ($\lesssim 0.01$ G) to be acceptable for this study because it is small compared with the inhomogeneous line width for methyl-PBN (≈ 1 G). These deviations are most likely explained by some small inaccuracy in the proton hyperfine parameters in the fitting model, some remaining scan inhomogeneity, and/or by insufficiently small digital steps in magnetic field for data sampling (25 mG). Better accuracy for very small $B_N^{94.5}$ might be achieved with deuterated nitroxides, which have a very small inhomogeneous width ($\lesssim 0.1$ G). It might be interesting to carry out some more studies of the picosecond-scale rotations of these nitroxide to determine whether the current theory fits the data well in this range. Overall, our discussion shows that (i) a nonsecular line width behavior can be observed at the W-band for some small spin adducts, such as methyl-PBN, and (ii) nonsecular terms become negligible if experimental $B_N^{94.5} > 0.1$ G.

Plots of parameters $A^{94.5}$ vs $B_N^{94.5}$ and $C_N^{9.5}$ vs $B_N^{9.5}$ for methyl-PBN and tetradecyl-PBN spin adducts can be well fitted by a straight line over the temperature/viscosity range when nonsecular terms can be neglected (*i.e.*, $B_N^{94.5} \gtrsim 0.1$ G). A plot of parameters $A^{94.5}$ vs $B_N^{94.5}$ and the linear regression for tetradecyl- and methyl-PBN spin adduct in toluene solvent are shown in Figure 6, A and B, respectively. The linear regression gives $A^{94.5}/B_N^{94.5} = 1.92$ and $C_N^{9.5}/B_N^{9.5} = 0.975$ for tetradecyl-PBN adduct and $A^{94.5}/B_N^{94.5} = 2.19$ and $C_N 9.5/B_N^{9.5} = 1.02$ for methyl-PBN adduct. These ratios and magnetic matrix parameters, listed in Table 1, were used to derive AVE's as described previously.[20,21,23] Calculated AVE's for both spin adducts are shown in Figure 7. Intersections of AVE's give anisotropy parameters for rotational diffusion of the spin adduct motion which are $\rho_x = 2.7 \pm 0.3$ and $\rho_y = 3.6 \pm 0.3$ for the methyl-PBN adduct and $\rho_x \approx \rho_y = 1.0 \pm 0.20$ for the tetradecyl-PBN

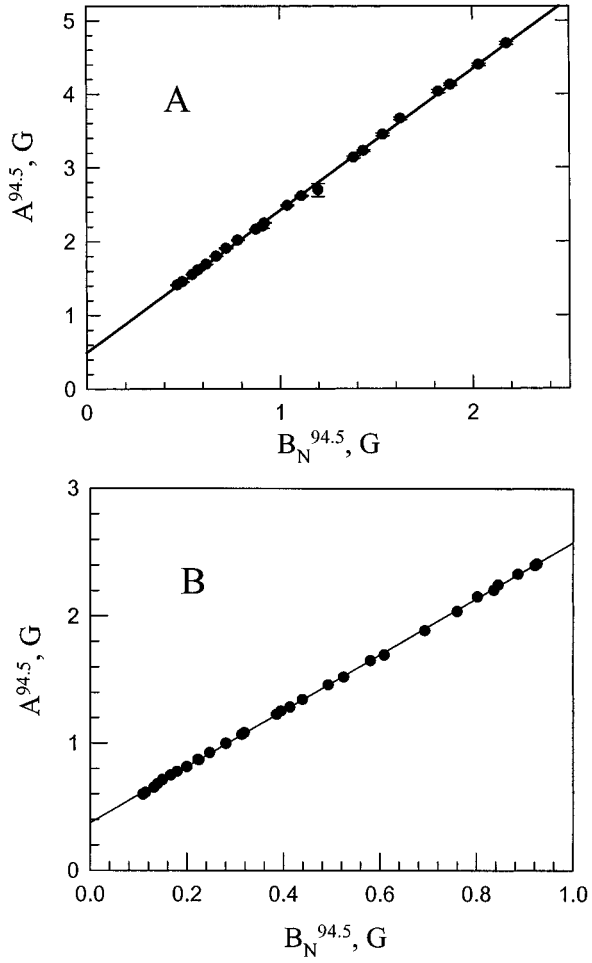

Figure 6. Line width parameters $A^{94.5}$ and $B_N^{94.5}$ measured at W-band for 0.1 mM toluene solution of tetradecyl-PBN (A) and a portion of methyl-PBN data for which nonsecular line width terms can be neglected (B). Solid lines are linear regressions of the data, characterized by a slope $A^{94.5}/B_N^{94.5} = 1.92$ for tetradecyl-PBN (A), and $A^{94.5}/B_N^{94.5} = 2.19$ G for methyl-PBN (B).

adduct. It is necessary to note that these parameters are calculated in the principal coordinate system of magnetic matrices, in which the *x* axis is along the N−O bond and the *z* axis is close to a perpendicular to the C−N−C plane. In this coordinate system, the *y* axis coincides most closely with the long axis of the molecule. Anisotropy parameters for methyl-PBN adduct indicate that rotational motion is fully anisotropic, with the fastest rotation around the *y* axis and slower rotations around the *x* and *z* axes. In contrast, results for tetradecyl-PBN show almost isotropic effective motion of the molecule in a nonpolar toluene solvent. A model for a configuration of tetradecyl-PBN in a polar solvent has been suggested by Yu *et al.*[27] in the conclusion of another study. These authors reported that, for PBN spin adducts formed by precursors with long alkyl chains ($n > 5$), the rate of ascorbate reduction decreases as alkyl chain length increases. It has been suggested that the long alkyl chain is "wrapped" around the molecule when in a polar solvent, effectively protecting NO group from the approaching ascorbate molecules and preventing the electron transport. For the tetradecyl-PBN adduct, such a configuration of the molecule may result in essentially isotropic rotational diffusion.

Data on rotational anisotropy parameters are necessary for accurate determination of rotational correlation time τ_R. (See definition of τ_R for fully anisotropic model given in ref 21.) For example, for toluene solution at $T = 260$ K, $\tau_R \approx 11 \times 10^{-12}$ s for methyl-PBN and $\tau_R \approx 78 \times 10^{-12}$ s for tetradecyl-PBN. These small τ_R values indicate that there is no aggregation

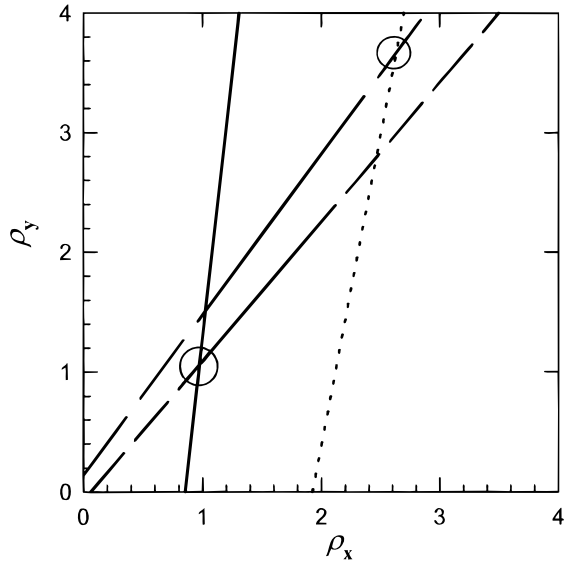

Figure 7. Determination of anisotropy parameters ρ_x and ρ_y: solid line, allowed value equation (AVE) for tetradecyl-PBN adduct, calculated from magnetic parameters and $A/B_N = 1.92$ as determined at W-band; medium-dashed line, AVE for tetradecyl-PBN adduct estimated from B_N/C_N as measured at W-band. Intersection (shown as a circle) gives $\rho_x = 1.0 \pm 0.2$ and $\rho_y = 1.0 \pm 0.2$ and characterizes the rotation of tetradecyl-PBN as essentially isotropic. Dotted line: AVE for methyl-PBN adduct, calculated from W-band data using $A/B_N = 2.19$; long-dash line: AVE calculated from B_N/C_N measured at X-band. Intersection (shown as a circle) gives $\rho_x = 2.7 \pm 0.3$ and $\rho_y = 3.6 \pm 0.3$.

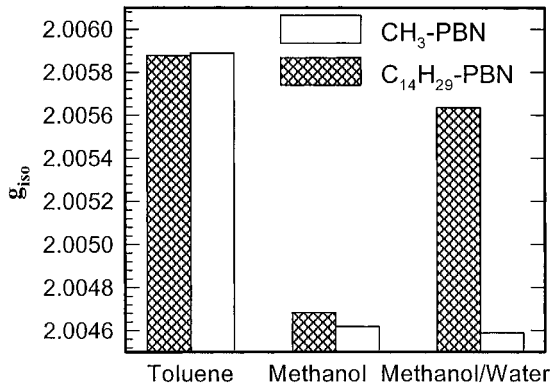

Figure 8. Experimental isotropic *g* factors for methyl- and tetradecyl-PBN adducts as measured at W-band (95 GHz) in toluene, methanol, and methanol/water mixture (7:3 volume ratio).

of the spin adducts in solution. The data on rotational correlation time can be used also to estimate broadening of EPR spectra from the spin adducts at other EPR frequencies.

The results demonstrate that for spin adducts with very similar magnetic parameters (**A** and **g** matrices) but different geometries, rotational anisotropy parameters can be strikingly different. Line width parameter *B*, as measured at high magnetic fields, can provide additional information for spin adduct identification, while anisotropy parameters of rotational diffusion tensors obtained from multifrequency EPR data give some insight into configuration of spin adduct molecules in solution.

High-frequency EPR, affording high accuracy in *g* factor measurements, allowed us to observe the changes in organization of spin adduct molecules with increased polarity of solution. As an example, we have measured g_{iso} for methyl- and tetradecyl-PBN spin adducts in toluene, methanol, and methanol/water mixture (7:3 volume ratio). The results are summarized in Figure 8. In toluene, g_{iso} for the two spin adducts proved to be almost equal (see also Table 2). In methanol, g_{iso} for

tetradecyl-PBN is slightly but measurably higher ($\Delta g = 6.6 \times 10^{-5}$) than for methyl-PBN. This may serve to indicate a lower charge in the vicinity of the free electron, *e.g.*,[28] perhaps caused by some steric protection by the long tetradecyl chain. In methanol/water mixture, we observed a further decrease in g_{iso} for methyl-PBN and attribute it to a higher polarity, while for tetradecyl-PBN adduct, g_{iso} was sharply increased. The last is a result of micelle formation, which was further confirmed by light scattering. Micelle formation for tetradecyl-PBN adduct in a methanol/water mixture cannot explain the essentially isotropic rotation observed for this spin adduct in toluene: toluene is essentially nonpolar, and the observed rotational correlation times rule out the possibility of adduct aggregation. The unique sensitivity of HF EPR to even small changes in g_{iso}, as it has been demonstrated here, needs to be exploited in other studies to track initial stages and critical concentrations of aggregation of hydrophobic residues of molecules in solutions, initial stages of micelle formation, and protein folding.

It is important to note that the accuracy of g_{iso} measurements given here corresponds to relative measurements. We have found that, at the same settings of the main field of the superconductive magnet, g_{iso} values were repeatable to at least 1 ppm. However, the absolute accuracy of the measurements is lower, mainly because of difficulties in accurately measuring magnetic field, especially inside the cavity. The absolute accuracy of g_{iso} measurements was estimated as 10−20 ppm. To improve the accuracy of relative g_{iso} measurements, we used aqueous solutions of deuterated Tempone to calibrate the magnetic field after resetting the main field of the superconductive magnet.

Conclusions

High-field EPR can be a valuable supplement to conventional (9.5 GHz) EPR for spin adduct characterization. Advantages of high-field EPR for characterization and differentiation of spin adducts have been demonstrated for solutions of individual spin adducts and spin adducts in mixtures. Enhanced *g* factor resolution at 95 GHz as compared to conventional 9.5 GHz EPR allows one to clearly separate signals arising from mixtures of phenyl- and trichloromethyl-PBN adducts in benzene. We have shown that at 95 GHz the gain in *g* factor resolution is sufficient to offset the line broadening caused by enhanced contributions from rotational modulation of the **g** matrix at high magnetic fields. For methyl-PBN in toluene it has been shown that these broadening effects in nonviscous solvents are small compared with the inhomogeneous line width. Thus, the *g* factor appears to be a newly useful parameter for spin adduct characterization. Because of enhanced sensitivity to fast rotational motion, high-field EPR gives more accurate estimation of rotational dynamics parameters and allows measurements of full diffusion tensors. Line width parameter *B* and rotational diffusion tensor characterize a molecule as a whole, providing data on configuration of the molecule; this can be used as additional information for spin adduct characterization.

Acknowledgment. This work used resources of the IERC (NIH P41-RR01811). Y.K. and E.G.J. acknowledge support from NIH (Grant P41-RR05517). R.B.C. and R.L.B. acknowledge support from NIH (Grant R01-GM42208). Support to T.S. was provided by a University of Illinois Fellowship. The authors are thankful to Prof. J. S. Hyde (Medical College of Wisconsin) for suggesting use of dynamics parameters as derived from HF EPR data for spin adduct identification.

References and Notes

(1) Degray, J. A.; Mason, R. P. Biological Spin Trappings In *Electron Spin Resonance*; The Royal Society of Chemistry: Cambridge, 1994; Vol. 14, Chapter 8, pp 246−301.

(2) Janzen, E. G. In *Free Radicals in Biology*; Pryor, W. A., Ed.; Academic Press: New York, 1980; Vol. 4, p 115.

(3) Kelman, D. J.; Mason, R. P. *Arch. Biochem. Biophys*. **1993**, *306*, 439.

(4) Perkins, M. J. *Adv. Phys. Org. Chem*. **1980**, *17*, 1.

(5) Li, A. S. W.; Chignell, C. F. J. *Biochem. Biophys. Methods* **1991**, *22*, 83.

(6) Rezska, K.; Bilski, P.; Sik, R. H.; Chignell,C. F. *Free Radical Res. Commun.* **1993**, *19*, S33.

(7) Janzen, E. G.; Zhang, Y.-K.; Haire, D. L. *Magn. Reson. Chem*. **1994**, *32*, 711.

(8) Rezska, K.; Chignell, C. F. *Free Radical Res. Commun.* **1991**, *14*, 97.

(9) Kotake, Y.; Okazaki, M.; Kuwata, K. *J. Am. Chem. Soc*. **1977**, *99*, 5198.

(10) Janzen, E. G.; Oehler, U. M.; Haire, D. L.; Kotake, Y. *J. Am. Chem. Soc*. **1986**, *108*, 6858.

(11) Janzen, E. G.; Chen, G.; Bray, T. M.; Rinke, L. A.; Poyer, J. L.; McCay, P. B. *J. Chem. Soc., Perkin Trans.* 2 **1993**, 1983.

(12) Morse II, P. D.; Magin, L.; Swartz, H. M. *Rev. Sci. Instrum.* **1985**, *56*, 94.

(13) Wang, W.; Belford, R. L.; Clarkson, R. B.; Davis, R. B.; Forrer, R. B.; Nilges, M. J.; Timken, M. D.; Watczak, T.; Thurnauer, M. C.; Norris, J. R.; Morris, A. L.; Zwang, Y. *Appl. Magn. Reson.* **1994**, *6*, 195.

(14) Ondar, M. A.; Grinberg, O. Ya.; Dubinskii, A. B.; Shestakov, A. F.; Lebedev, Ya. S. *Khim. Fiz.* **1983**, *2*, 54.

(15) Ondar, M. A.; Grinberg, O. Ya.; Dubinskii, A. B.; Lebedev, Ya. S. *Sov. J. Chem. Phys.* **1985**, *3*, 781.

(16) Nilges, M. J. Ph.D. Thesis, University of Illinois, 1979.

(17) Smirnov, A. I.; Belford, R. L. *J. Magn. Reson.* A **1995**, *113*, 65.

(18) Janzen, E. G.; Coulter, G. A.; Oehler, U. M.; Bergsma, J. P. *Can. J. Chem.* **1982**, *60*, 2725.

(19) Lebedev, Ya. S. In *Modern Pulsed and Continuous-Wave Electron Spin Resonance*; Kevan, L., Bowman, M. K., Eds.; John Wiley & Sons: New York, 1990; Chapter 8.

(20) Earle, K. A.; Budil, D. E.; Freed, J. H. *J. Phys. Chem.* **1993**, *97*, 13289.

(21) Budil, D. E.; Earle, K. A.; Freed, J. H. *J. Phys. Chem.* **1993**, *97*, 1294.

(22) Smirnova, T. I.; Smirnov, A. I.; Clarkson, R. B.; Belford, R. L. *J. Phys. Chem*. **1995**, *99*, 9008.

(23) Kowert, B. A. *J. Phys. Chem.* **1981**, *85*, 229.

(24) Smirnov, A. I.; Smirnova, T. I.; Morse II, P. D. *Biophys. J*. **1995**, *68*, 2350.

(25) Brustolon, A. ; Maniero, M. L.; Ottaviani, M. F.; Romanelli, M.; Serge, U. *J. Phys. Chem.* **1990**, *94*, 6589.

(26) Goldman, S. A.; Bruno, G. V.; Freed, J. H. *J. Chem. Phys.* **1973**, *59*, 3071.

(27) Yu, Z.; Kotake, Y.; Janzen, E. G. *Redox Rep*. **1996**, *2*, 133.

(28) Griffith, O. H.; Jost, P. C. In *Spin Labeling*; Berliner, L. J., Ed.; Academic Press: New York, 1976; Chapter 12.